

racemization of the chiral center, the secondary alcohol at the point of attachment of the farnesylethyl side chain to the macrocycle of heme *a*, can occur under acidic conditions and possibly under basic conditions also, and this is due to the electron-withdrawing effect of the formyl group. Whether there is racemization of the porphyrin *o* chiral center during the preparation process is not known at this stage, but the dehydration of the secondary alcohol that happened with porphyrin *o* appears to be more facile than expected. The replacement of the formyl group with a methyl group at position 18 would certainly decrease the acidity of the  $\alpha$ -proton of the secondary alcohol, and might thus lead only to the elimination of a  $\beta$ -proton in the form of dehydration.

The farnesyl group present in heme *a* and heme *o* may have important roles for both hemes in their biological functions about which we can only speculate. One possible role of this side chain is to act as a lipophilic anchor holding the heme in the proper position within the membrane protein. Such a role for a hydrophobic tail appears to occur for the chlorophyll side chain in the photosynthetic reaction center.<sup>21</sup> Other roles could be related to electron transfer.<sup>13</sup> Woodruff et al.<sup>22</sup> recently proposed that one of the unsaturated isoprenoid groups of the farnesyl chain might alternatively coordinate heme iron and the nearby Cu ion in *aa*<sub>3</sub>-type cytochrome *c* oxidases, and that such coordination might play a significant role in redox-linked proton translocation.

(21) Michel, H.; Diesenhofer, J. *Biochemistry* 1988, 27, 1.

(22) Woodruff, W. H.; Einarsdóttir, Ó.; Dyer, R. B.; Bagley, K. A.; Palmer, G.; Atherton, S. J.; Goldbeck, R. A.; Dawes, T. D.; Kligler, D. S. *Proc. Natl. Acad. Sci. U.S.A.* 1991, 88, 2588-2592.

The finding by Puustinen et al.<sup>23</sup> that the cytochrome *o* oxidase is also proton-translocating is consistent with this idea. Considering the close structural resemblance between these hemes, it is possible that they are related in biosynthesis. Very few studies on the biosynthesis of heme *a* are recorded in the literature, but it is generally believed that protoporphyrin IX is the biogenetic precursor.<sup>24</sup> A likely mechanism for formation of the side chain at C-3 that uses farnesyl pyrophosphate has been proposed.<sup>25</sup> Clezy and Fookes<sup>26</sup> reported a decade ago the synthesis of **1b** as a possible precursor of heme *a*. At that time it was not realized that **1a** itself is a prosthetic group of a natural quinol oxidase. Even now, we are not certain if porphyrin *o* is indeed an intermediate in the biosynthetic pathway of heme *a*, that is, whether it lies between protoporphyrin and porphyrin *a*. This seems to be a worthwhile objective to pursue in the future.

**Acknowledgment.** This work was supported by the NIH Grants GM 34468 and 36520 (C.K.C.) and GM 25480 (G.T.B.), the Sigrid Jusélius Foundation, and the Academy of Finland (M.W.). The NMR data were obtained on instrumentation purchased in part with funds from NIH Grant 1-S10-RR04750-01 and from NSF Grant CHE 88-00770.

(23) Puustinen, A.; Finel, M.; Virkki, M.; Wikström, M. *FEBS Lett.* 1989, 249, 163-167.

(24) Weinstein, J. D.; Branchaud, R.; Beale, S. I.; Bement, W. J.; Sinclair, P. R. *Arch. Biochem. Biophys.* 1986, 245, 44.

(25) Leeper, F. J. *Nat. Prod. Rep.* 1985, 2, 19-47.

(26) Clezy, P. S.; Fookes, C. J. R. *Aust. J. Chem.* 1981, 34, 871-883.

## Spectroscopic Studies of *p*-(*N,N*-Dimethylamino)benzotrile and Ethyl *p*-(*N,N*-Dimethylamino)benzoate in Supercritical Trifluoromethane, Carbon Dioxide, and Ethane

Ya-Ping Sun,<sup>†</sup> Marye Anne Fox,<sup>\*,†</sup> and Keith P. Johnston<sup>\*,†</sup>

Contribution from the Departments of Chemistry and Chemical Engineering, The University of Texas at Austin, Austin, Texas 78712. Received July 29, 1991

**Abstract:** Absorption and emission spectral maxima, bandwidths, and fractional contribution of twisted intramolecular charge transfer states to the observed emission of *p*-(*N,N*-dimethylamino)benzotrile (DMABN) and ethyl *p*-(*N,N*-dimethylamino)benzoate (DMAEB) in supercritical CHF<sub>3</sub>, CO<sub>2</sub>, and C<sub>2</sub>H<sub>6</sub> are presented. By examining a wide range of reduced densities from 0.05 to 2.2, we have discovered a characteristic density dependence in the spectral shifts in all three fluids. A model for these spectral effects is proposed, differentiating intermolecular interactions in three distinct regions: gas-phase solute-solvent clustering, clustering in the near-critical region, and "liquidlike" solvation. Even below a reduced density of 0.5, clustering of solvent about solute is already prevalent.

### Introduction

Molecular spectroscopy in supercritical fluids is a relatively new research subject, since the utility of this medium in probing solvent effects on photophysical phenomena has only recently been recognized.<sup>1-11</sup> Solvent friction, polarity, and clustering effects, which are very important in this regard both experimentally and theoretically,<sup>12-14</sup> are particularly amenable to study in supercritical fluids. The unique feature of a supercritical fluid is that its solvation properties can be continuously varied over a wide range, making it possible to probe solute-medium interactions without changing solvent. The density of a supercritical fluid is lower than the bulk density of the liquid phase, but larger than what is usually

encountered in clusters in a supersonic jet expansion. Spectroscopic studies in supercritical fluids of various solute probes can therefore

(1) Okada, T.; Kobajashi, Y.; Yamasa, H.; Mataga, N. *Chem. Phys. Lett.* 1986, 128, 583.

(2) Kim, S.; Johnston, K. P. *Ind. Eng. Chem. Res.* 1987, 26, 1206.

(3) Kim, S.; Johnston, K. P. *AIChE J.* 1987, 33, 1603.

(4) Kajimoto, O.; Futakami, M.; Kobayashi, T.; Yamasaki, K. *J. Phys. Chem.* 1988, 92, 1347.

(5) Yonker, C. R.; Smith, R. D. *J. Phys. Chem.* 1988, 92, 235.

(6) Hrnjez, B. J.; Yazdi, P. T.; Fox, M. A.; Johnston, K. P. *J. Am. Chem. Soc.* 1989, 111, 1915.

(7) Brennecke, J. F.; Eckert, C. A. *Am. Chem. Soc. Symp. Ser.* 1989, 406, 14. Brennecke, J. F.; Tomasko, D. L.; Peshkin, J.; Eckert, C. A. *Ind. Eng. Chem. Res.* 1990, 29, 1682.

(8) Johnston, K. P.; Kim, S.; Combes, J. *Am. Chem. Soc. Symp. Ser.* 1989, 406, 52.

<sup>†</sup>Department of Chemistry.

<sup>†</sup>Department of Chemical Engineering.

be an effective means to understand clustering in terms of solute-solvent interactions. (Here, clustering refers to the local density augmentation of solvent molecules about the solute molecule.<sup>2,11,15,16</sup>) The supercritical fluid also serves as a medium for the observation of some quite unique phenomena, such as the so-called "Kramers turnover" in the medium viscosity dependence of photoisomerization.<sup>17</sup>

Molecules which form twisted intramolecular charge transfer (TICT) states are particularly good for examining solvation effects. It is well established<sup>18</sup> that the TICT state is a highly polar excited state, very sensitive to medium polarity and polarizability. The dual fluorescence often observed in these molecules makes a study of their solvatochromic effects easy and accurate. Recently, molecules forming TICT states have also been used as models for transient solvation dynamics on ultrafast time scales.<sup>14</sup>

*p*-(*N,N*-Dimethylamino)benzotrile (DMABN) is a prototypical precursor for a TICT state. Kajimoto and co-workers have studied the absorption and fluorescence of DMABN in supercritical trifluoromethane at 50 °C up to a density of ~0.7 g/mL,<sup>4</sup> where the observed solvatochromic effects deviate significantly from those expected by the Onsager reaction field model.<sup>19,20</sup> With extension of this study to the absorption spectra of DMABN in supercritical ethane at 50 °C up to a density of ~0.2 g/mL, similar deviations were observed.<sup>9</sup> These unusual solvatochromic effects, also observed in other systems,<sup>21-23</sup> were interpreted as simple aggregation in which the solute molecule clusters with several solvent molecules.<sup>2-4,8,9</sup>

Although these approaches appear to be able to account for available experimental observations of DMABN qualitatively, the validity of these interpretations is still in question. After all, these analyses were based on rather limited experimental observations, primarily in the low-density region. The overall solvatochromic behavior of DMABN in ethane, for example, is not clear even experimentally because data for the postcritical density region are not available, let alone an applicable theoretical modeling. A more complete study is necessary before any definite conclusions can be made.

In the treatment of solvent effects on DMABN and other molecules, the bathochromic (red) absorption spectral shifts in both CHF<sub>3</sub> and ethane were usually attributed solely to the differences of solvation of the ground and excited states,<sup>24</sup> namely, that the excited state is more stabilized by solvation than the ground state because of its larger dipole moment. Such energetic changes should, in principle, be reflected in the emission also. Since it has been proposed<sup>18,25</sup> that DMABN and ethyl *p*-(*N,N*-

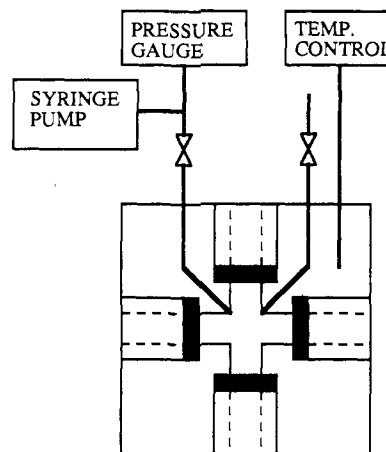


Figure 1. Experimental apparatus.

dimethylamino)benzoate (DMAEB) have different state orderings on their excited-state potential energy surfaces, a thorough study of solvatochromic effects on both absorption and emission may provide valuable insight into such intermolecular interactions.

While the formation of a TICT state in DMABN has been well established,<sup>18,26,27</sup> despite a few recent arguments,<sup>28-32</sup> the situation for DMAEB seems less clear in the literature. A mechanism that involves formation of a 1:1 exciplex between DMAEB and a solvent molecule in dioxane or other polar solvents has been proposed.<sup>33</sup> An attempt has also been made to extend this mechanism to include other compounds such as DMABN.<sup>29</sup> The mechanism assumes that in nonpolar hydrocarbon solvents the emission of DMAEB is from the locally excited Franck-Condon state, and in dioxane or polar solvents the dual fluorescence is from two kinds of 1:1 solute-solvent exciplexes (one in a near-planar geometry and the other in a twisted geometry) in thermodynamic equilibrium. Although the mechanism appears to be able to explain the limited experimental results for DMAEB, the assumption that even the planar DMAEB forms a 1:1 exciplex with solvent is highly questionable. For DMABN, it has been shown<sup>32</sup> that a DMABN-solvent 1:1 cluster formed in a superionic expansion does not have dual fluorescence, implying that TICT state formation requires solvation of the solute by more than one solvent molecule. Our results for DMAEB in supercritical fluids are also at odds with the 1:1 exciplex assumption. A delayed fluorescence mechanism, which better accounts for available experimental observations of DMABN and DMAEB, is proposed instead.

In a preliminary report from our research group<sup>6</sup> on DMAEB in trifluoromethane, we attempted to use steady-state fluorescence to probe the possible inhomogeneous distribution of solute-solvent clusters in the near-critical region. In this paper, we report a comprehensive study of DMABN and DMAEB in both polar (CHF<sub>3</sub>) and nonpolar (CO<sub>2</sub> and ethane) supercritical fluids over a considerably wider density range than in previous studies. By using these TICT state forming molecules as probes, characteristic solute-solvent interactions are examined spectroscopically. A model is presented to explain the intermolecular interactions at gaslike, near-critical, and liquidlike densities. The unusual sol-

- (9) Morita, A.; Kajimoto, O. *J. Phys. Chem.* **1990**, *94*, 6420.  
 (10) Betts, T. A.; Bright, F. V. *Appl. Spectrosc.* **1990**, *44*, 1196, 1203.  
 (11) Betts, T. A.; Zagrobelny, J.; Bright, F. V. *Am. Chem. Soc. Symp. Ser.* **1991**, in press.  
 (12) Saltiel, J.; Sun, Y.-P. In *Photochromism. Molecules and Systems*; Dürr, H., Bouas-Laurent, H., Eds.; Elsevier: Amsterdam, 1990; p 64.  
 (13) Waldeck, D. H. *Chem. Rev.* **1991**, in press.  
 (14) Barbara, P. F.; Jarzaba, W. *Adv. Photochem.* **1990**, *15*, 1.  
 (15) Johnston, K. P.; McFunn, G. J.; Peck, D. G.; Lemert, R. M. *Fluid Phase Equilib.* **1989**, *52*, 337.  
 (16) Debenedetti, P. G. *Chem. Eng. Sci.* **1987**, *42*, 2203.  
 (17) Lee, M.; Holtom, G. R.; Hochstrasser, R. M. *Chem. Phys. Lett.* **1985**, *118*, 359.  
 (18) Rettig, W. *Angew. Chem., Int. Ed. Engl.* **1986**, *25*, 971.  
 (19) Onsager, L. *J. Am. Chem. Soc.* **1936**, *58*, 1486.  
 (20) Mataga, N.; Kubota, T. *Molecular Interactions and Electronic Spectra*; Marcel Dekker: New York, 1970.  
 (21) Frye, S. L.; Yonker, C. R.; Kalkwarf, D. R.; Smith, R. D. *Am. Chem. Soc. Symp. Ser.* **1987**, *329*, 27.  
 (22) Gehrke, C.; Schroeder, J.; Schwarzer, D.; Troe, J.; Voss, F. *J. Chem. Phys.* **1990**, *92*, 4805.  
 (23) Schroeder, J.; Schwarzer, D.; Troe, J.; Voss, F. *J. Chem. Phys.* **1990**, *93*, 2393.  
 (24) Birks, J. B. *Photophysics of Aromatic Molecules*; Wiley-Interscience: London, 1970.  
 (25) Rettig, W.; Wermuth, G.; Lippert, E. *Ber. Bunsen-Ges. Phys. Chem.* **1979**, *83*, 692.

- (26) Rotkiewicz, K.; Grellman, K. H.; Grabowski, Z. R. *Chem. Phys. Lett.* **1973**, *19*, 315.  
 (27) Lippert, E.; Rettig, W.; Bonacic-Koutecky, V.; Heisel, F.; Mische, J. A. *Adv. Chem. Phys.* **1987**, *68*, 1.  
 (28) Visser, R. J.; Varma, C. A. G. O.; Konijnenberg, J.; Bergwerf, P. J. *Chem. Soc., Faraday Trans. 2* **1983**, *79*, 347.  
 (29) Weisenborn, P. C. M.; Huizer, A. H.; Varma, C. A. G. O. *Chem. Phys.* **1988**, *126*, 425.  
 (30) Cazeau-Dubroca, C.; Lyazidi, S. A.; Nouchi, G.; Peirigua, A. *Nouv. J. Chim.* **1986**, *10*, 337.  
 (31) Pilloud, D.; Suppan, P.; van Haelst, L. *Chem. Phys. Lett.* **1987**, *137*, 130.  
 (32) Kobayashi, T.; Futakami, M.; Kajimoto, O. *Chem. Phys. Lett.* **1986**, *130*, 63.  
 (33) Visser, R. J.; Varma, C. A. G. O.; Weisenborn, P. C. M.; Warman, J. M.; de Haas, M. P. *Chem. Phys. Lett.* **1985**, *113*, 330.

Table I. Critical Parameters of CHF<sub>3</sub>, CO<sub>2</sub>, and C<sub>2</sub>H<sub>6</sub>

	$t_c$ (°C)	$P_c$ (psia)	$\rho_c$ (mol/dm <sup>3</sup> )
CHF <sub>3</sub>	25.6	702.7	7.51
CO <sub>2</sub>	31.0	1071	10.63
C <sub>2</sub> H <sub>6</sub>	32.2	706.5	6.88

vatochromic behavior of DMABN and DMAEB in supercritical fluids is discussed in terms of solvation and clustering effects on their excited-state potential energy surfaces.

### Experimental Section

**Materials.** DMABN (Aldrich, 98%) and DMAEB (Aldrich, 99%) were both repeatedly recrystallized from ethanol/water before being stored under vacuum for at least 12 h. Trifluoromethane (Linde Halocarbon 23, 98%), carbon dioxide (Liquid Carbonic, 99.99%), and ethane (Big Three Gases, CP grade) were purified with a freshly packed column of activated carbon. In addition, trifluoromethane was passed through a silica gel column. Research grade trifluoromethane (MG Industry) was also used as received.

**Measurements.** Absorption spectra were recorded on a Cary 2300 absorption spectrophotometer. Fluorescence spectra were measured on an SLM Amico SPF-500C emission spectrophotometer equipped with a 300-W Xe lamp using a right-angle geometry. Both instruments are interfaced to personal computers. The high-pressure fluorescence experiments were conducted in a 3-in. cubic stainless steel cell, Figure 1. A  $5/8$ -in.-diameter by  $1/10$ -in.-thick sapphire window was inserted into each of the four  $5/16$ -in. channels, and a seal was made with a Teflon O-ring. This cell can withstand pressures of at least 5000 psia. Pressure was generated by a syringe pump and was measured on a Heise pressure gauge. The cell temperature was maintained constant ( $\pm 0.1$  °C for temperatures close to room temperature and  $\pm 0.2$  °C for higher temperatures) by a pair of cartridge heaters, a platinum resistance thermometer, and an Omega RTD temperature controller. Absorption spectra were obtained either in the cell described above or in a high-pressure UV cell with two sapphire windows.<sup>2</sup>

A hexane solution of known optical density was loaded into the cell. The hexane solvent was evaporated under a slow stream of nitrogen gas. Spectra at low supercritical fluid densities were collected using the multiple-averaging mode of the instrument. In order to enhance the S/N ratio for the weak absorption and emission spectra at low densities, the measurements were repeated, and then averaged on a personal computer. All emission spectra were corrected for nonlinear instrumental response.

The densities of the supercritical fluids were calculated from observed pressures using multiparameter equations of state for CHF<sub>3</sub>,<sup>34,35</sup> CO<sub>2</sub>,<sup>36</sup> and ethane.<sup>37</sup> Since these equations are pressure explicit, an iterative computational method was used. The density-dependent properties are shown on a reduced density  $\rho_r$  scale, defined as the ratio of density  $\rho$  to the critical density  $\rho_c$ ,  $\rho_r = \rho/\rho_c$ . The critical parameters for CHF<sub>3</sub>, CO<sub>2</sub>, and ethane are listed in Table I.

**Deconvolution of Dual Fluorescence.** The emission spectra of the TICT state were deconvoluted from the total emission on the basis of the assumptions that the locally excited state (LE) emission band only shifts bathochromically with increasing CO<sub>2</sub> density, but does not change its shape, and that the TICT emission band is Gaussian:

$$I(\bar{\nu}) = x_{LE} I_{LE}(\bar{\nu} + \Delta\bar{\nu}) + x_{TICT} \{ (a/\pi)^{1/2} \exp[-a(\bar{\nu} - \bar{\nu}_{max}^{TICT})^2] \} \quad (1)$$

where  $I_{LE}(\bar{\nu})$  is the intensity of the emission spectrum at very low solvent density, consisting of the LE emission band only,  $\bar{\nu}_{max}^{TICT}$  is the TICT band maximum, and  $a$  is inversely proportional to the square of the full width at half-maximum (fwhm). A bathochromic shift of the LE emission band in a spectral mixture is represented by  $\Delta\bar{\nu}$ , so that  $\Delta\bar{\nu}$  is a function of CO<sub>2</sub> density. An iterative approach was used for the nonlinear least-squares fitting. Each observed spectrum was fitted by eq 1 with three adjustable parameters,  $x_{LE}$ ,  $\bar{\nu}_{max}^{TICT}$ , and  $a$ , at a given  $\Delta\bar{\nu}$  value. A best fit was achieved by gradually varying  $\Delta\bar{\nu}$ , corresponding to red-shifting the pure LE emission band, until the minimum of fitting standard deviation is reached.

A somewhat different approach was used for spectral deconvolution in CHF<sub>3</sub>. The dual fluorescence could be well approximated by two

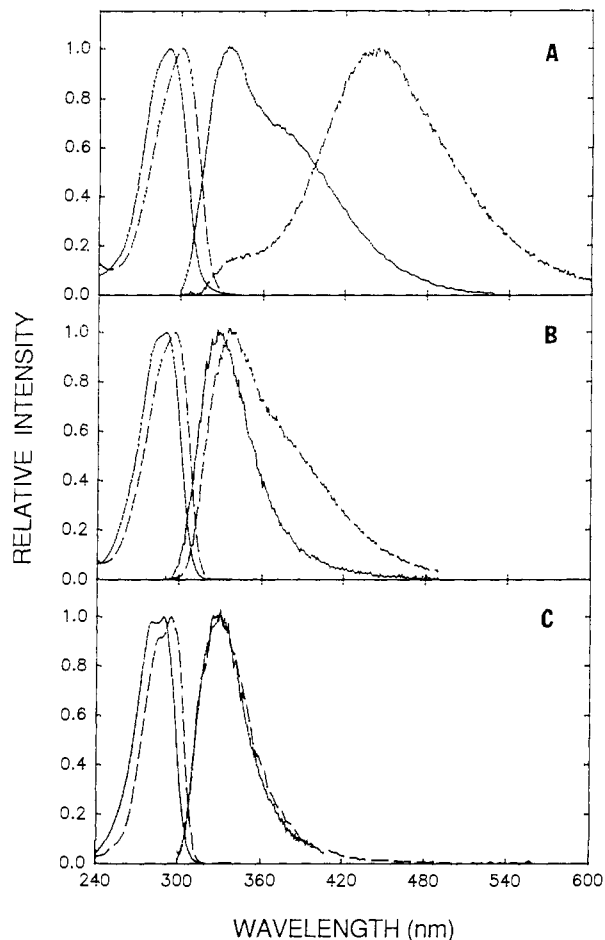


Figure 2. Absorption (left) and fluorescence (right) spectra of DMAEB in supercritical (A) CHF<sub>3</sub>, (B) CO<sub>2</sub>, and (C) ethane. The solid and dashed lines represent spectra at low ( $\rho_r < 0.4$ ) and high ( $\rho_r > 1.8$ ) densities, respectively.

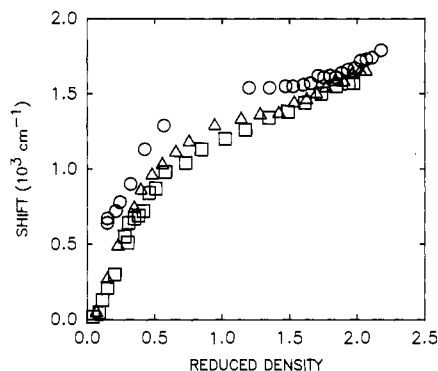


Figure 3. Bathochromic shifts of the DMAEB absorption spectral maximum (relative to the absorption spectral maximum in absence of solvent, 285.5 nm) induced by changes in the reduced density of CHF<sub>3</sub> at 30.0 °C (○), 44.7 °C (△), and 59.6 °C (□). The critical density is at  $\rho_r = 1$ .

Gaussian functions,  $G_{LE}(\bar{\nu} - \bar{\nu}_{max}^{LE})$  and  $G_{TICT}(\bar{\nu} - \bar{\nu}_{max}^{TICT})$ , even at very low CHF<sub>3</sub> densities:

$$I(\bar{\nu}) = x_{LE} G_{LE}(\bar{\nu} - \bar{\nu}_{max}^{LE}) + x_{TICT} G_{TICT}(\bar{\nu} - \bar{\nu}_{max}^{TICT}) \quad (2)$$

where  $\bar{\nu}_{max}^{LE}$  is the LE band maximum.

### Results

Absorption and fluorescence of DMABN and DMAEB were measured isothermally in supercritical trifluoromethane, carbon dioxide, and ethane over a wide range of pressures up to 5000 psia (34.5 MPa).

**DMAEB in CHF<sub>3</sub>.** The absorption spectra of DMAEB were measured at 30.0, 44.7, and 59.6 °C. Shown in Figure 2A are

(34) Aizpiri, A. G.; Rey, A.; Davila, J.; Rubio, R. G.; Zollweg, J. A.; Streett, W. B. *J. Phys. Chem.* **1991**, *95*, 3351.

(35) Rubio, R. G.; Zollweg, J. A.; Streett, W. B. *Ber. Bunsen-Ges. Phys. Chem.* **1989**, *93*, 791.

(36) Benedict, M.; Webb, G. B.; Rubin, L. C. *Chem. Eng. Prog.* **1951**, *47*, 419.

(37) Younglove, B. A.; Ely, J. F. *J. Phys. Chem. Ref. Data* **1987**, *16*, 577.

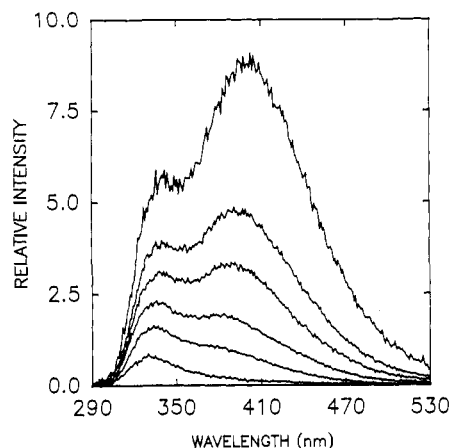


**Figure 4.** Dependence of the total emission intensities and the contribution of the TICT band on  $\text{CHF}_3$  density at 28.0 °C. From the bottom,  $\rho = 0.32, 0.47, 0.87, 1.09, 1.25,$  and  $1.60 \text{ mol/dm}^3$ .

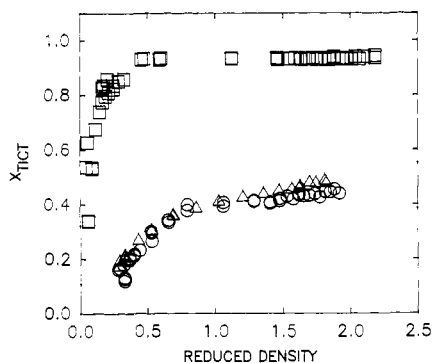


**Figure 5.** Fractional contribution of the TICT state emission of DMAEB as a function of the reduced solvent density in  $\text{CHF}_3$  at 28.0 °C ( $\square$ ), in  $\text{CO}_2$  at 33.8 °C ( $\circ$ ), and in  $\text{CO}_2$  at 49.7 °C ( $\Delta$ ).

representative spectra observed at low (solid line) and high (dashed) pressures. While the shape of the absorption band depends only weakly on fluid density, the spectral maximum shifts significantly to the red as  $\text{CHF}_3$  density increases. The dependence of the observed absorption maximum on the reduced density of  $\text{CHF}_3$  at temperatures above the critical temperature are shown in Figure 3. At all three temperatures, the shifts are large initially in the low-density region, and then level off just before the critical density.

The fluorescence spectra were measured at 28.0 °C. Our ability to reproduce our previous observation<sup>6</sup> of excitation wavelength dependence depends on the source of  $\text{CHF}_3$  and may be attributed to trace impurities in the solvent. The fluorescence spectra of DMAEB in rigorously purified  $\text{CHF}_3$  are essentially excitation wavelength independent at both low and high  $\text{CHF}_3$  densities.

The TICT emission starts at very low  $\text{CHF}_3$  density and grows rapidly in intensity, Figure 4, until a  $\rho_r$  of  $\sim 0.5$  where the relative intensity of the TICT band becomes essentially constant to a  $\rho_r$  of  $\sim 2.2$ , the upper limit of our apparatus. The total emission spectra were deconvoluted into contributions of the LE emission band and the TICT emission band, as described in the Experimental Section. The fractional contribution of the TICT band as a function of the reduced density of  $\text{CHF}_3$  is shown in Figure 5.  $x_{\text{TICT}}$  increases very rapidly in the low-density region, and then forms a plateau with an average value of  $\sim 0.93$ . As the density increases, the TICT band maximum also shifts to the red, in the same fashion as the intensity: an initial period of large shifts, followed by almost a plateau (Figure 6). The TICT bandwidth similarly depends on the  $\text{CHF}_3$  density, decreasing rapidly until a  $\rho_r$  of 0.5 or so, Figure 7. Outside this region, the bandwidth is essentially independent of the solvent density ( $\text{fwhm} = \sim 5250 \text{ cm}^{-1}$ ).

**DMABN in  $\text{CHF}_3$ .** Absorption spectra of DMABN were measured at 28.0 and 59.7 °C. At both temperatures the ab-

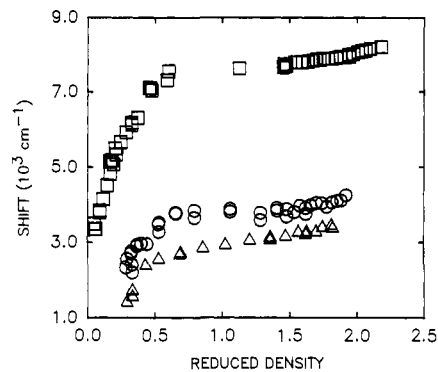


**Figure 6.** Bathochromic shifts of  $\lambda_{\text{max}}^{\text{TICT}}$  (relative to the LE band maximum in the absence of solvent, 330 nm) of DMAEB as a function of the reduced solvent density in  $\text{CHF}_3$  at 28.0 °C ( $\square$ ), in  $\text{CO}_2$  at 33.8 °C ( $\circ$ ), and in  $\text{CO}_2$  at 49.7 °C ( $\Delta$ ).

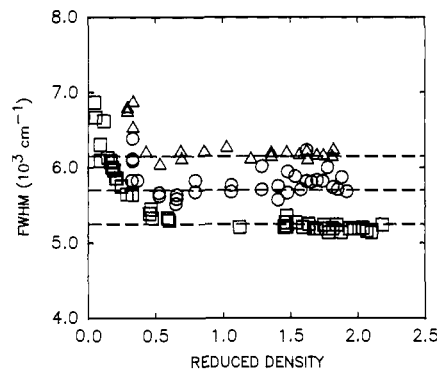


**Figure 7.** Dependence of the TICT band fwhm of DMAEB on the reduced solvent density in  $\text{CHF}_3$  at 28.0 °C ( $\square$ ), in  $\text{CO}_2$  at 33.8 °C ( $\circ$ ), and in  $\text{CO}_2$  at 49.7 °C ( $\Delta$ ).

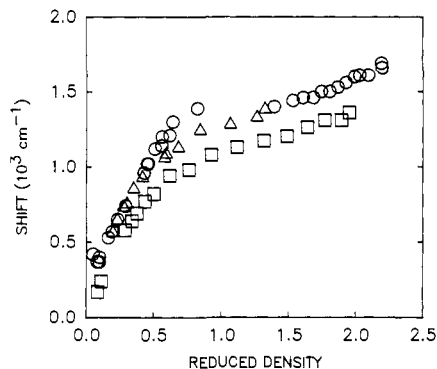


**Figure 8.** Bathochromic shifts of the DMABN absorption spectral maximum (relative to the absorption spectral maximum in absence of solvent, 270.5 nm) induced by changes in the reduced density of  $\text{CHF}_3$  at 28.0 °C ( $\circ$ ) and 59.7 °C ( $\square$ ). Also shown are the literature values for DMABN in  $\text{CHF}_3$  at 50 °C ( $\Delta$ ).<sup>4</sup>

sorption spectral maximum shifts to the red as the solvent density increases, in the same fashion as that observed in DMAEB. The initial large bathochromic shifts in the low-density region are less pronounced at high temperature than at low temperature, Figure 8. Also shown in the figure are the literature data at 50 °C,<sup>4</sup> which only extend to approximately the critical density.

Although the absorption spectra of DMABN and DMAEB are different, the dependencies of observed spectral bathochromic shifts on the  $\text{CHF}_3$  density are nearly identical.

**DMAEB in  $\text{CO}_2$ .** The absorption spectra of DMAEB at 33.8 °C (Figure 2B) shift bathochromically with increasing  $\text{CO}_2$  density, in parallel with the shifts in  $\text{CHF}_3$ . However, the initial rapid shifts in the low-density region are much smaller than those in  $\text{CHF}_3$ , Figure 9. After a plateau near the critical density of  $\text{CO}_2$ , the bathochromic shift continues to higher densities with a smaller slope than in the low-density region.

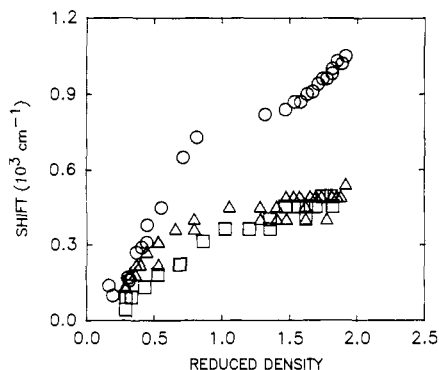


**Figure 9.** A comparison between the bathochromic shifts of the absorption (O, 33.8 °C) and of the emission ( $\Delta$ , 33.8 °C;  $\square$ , 49.7 °C) for DMAEB in CO<sub>2</sub>. The reference spectral maxima in the absence of solvent appear at 285.5 and 330 nm for absorption and emission, respectively.

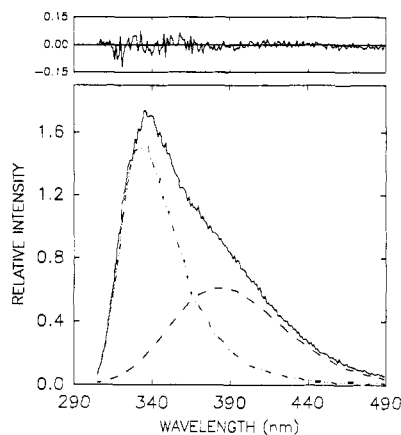


**Figure 10.** Deconvolution of the LE fluorescence (---) and the TICT fluorescence (---) from the total emission spectrum (—) for DMAEB in CO<sub>2</sub> at 33.8 °C ( $\rho = 20.4 \text{ mol/cm}^3$ ). The top inset represents the residual emission.

The fluorescence spectra similarly change continuously with CO<sub>2</sub> density. The LE emission band also shifts bathochromically, in parallel with the absorption band. As the density increases, the contribution of the TICT emission grows, eventually becoming a shoulder at  $\sim 380 \text{ nm}$  (Figure 2B). As in CHF<sub>3</sub>, no excitation wavelength dependence was observed.

The TICT emission band was deconvoluted from the total emission. Excellent fits of experimental spectra (Figure 10) confirm the validity of eq 1. The spectral shifts of the deconvoluted LE emission band at 33.8 and 49.7 °C are plotted against the reduced density of CO<sub>2</sub> in Figure 9. Apparently, the bathochromic shifts are smaller in the LE emission than in absorption. In contrast, the TICT band is much more sensitive to the solvent density, Figure 6. While the bathochromic shifts of the TICT band at the two temperatures are almost parallel in the region near or higher than the critical density, the shifts are smaller at 49.7 °C than at 33.8 °C in the low-density region. The same is true for a comparison of the bathochromic shifts of DMAEB in CHF<sub>3</sub> and in CO<sub>2</sub>.

The fractional contributions of the TICT emission ( $x_{\text{TICT}}$ ) are shown in Figure 5. The  $x_{\text{TICT}}$  changes with increasing solvent density in the same fashion as the bathochromic shift of  $\bar{\nu}_{\text{max}}^{\text{TICT}}$ . At the same density, the  $x_{\text{TICT}}$  is somewhat larger at 49.7 °C than at 33.8 °C.

Shown in Figure 7 are plots of the TICT bandwidth against density. Despite expected uncertainties in the low-density region, in which the TICT emission is weak, the data clearly indicate the trend of decreasing bandwidth at low densities, followed by a plateau. The pattern is the same as that observed in CHF<sub>3</sub>. At the plateau, the average TICT bandwidth at 49.7 °C ( $\sim 6150 \text{ cm}^{-1}$ ) is substantially larger than that at 33.8 °C ( $\sim 5700 \text{ cm}^{-1}$ ).

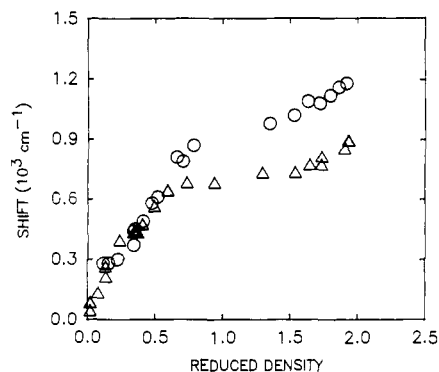


**Figure 11.** A comparison between the bathochromic shifts of the absorption (O) and of the emission ( $\Delta$ ) for DMABN in CO<sub>2</sub>. The reference spectral maxima in absence of solvent appear at 270.5 and 337 nm for absorption and emission, respectively.

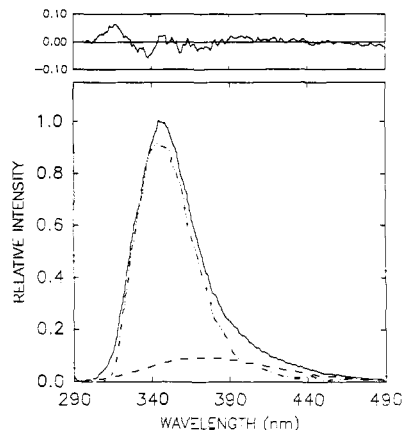


**Figure 12.** An attempted deconvolution of DMABN fluorescence spectrum in CO<sub>2</sub> at 33.8 °C (—) into the LE emission band (---) and a Gaussian (---), probably due to the TICT state emission. The top inset represents the residual emission.

**DMABN in CO<sub>2</sub>.** The absorption spectra of DMABN at 33.8 °C undergo similar bathochromic shifts with increasing CO<sub>2</sub> density, Figure 11. The dependence of the shift on density for DMABN is identical to that for DMAEB.

The fluorescence spectra of DMABN were measured at 33.8 °C as a function of CO<sub>2</sub> density. The spectral maximum also undergoes bathochromic shifts with increasing CO<sub>2</sub> density, Figure 11. The shifts were obtained without deconvolution because the contribution of the TICT state emission, if any, is insignificant. As CO<sub>2</sub> density increases, there is a weak extra emission at the red onset of the LE band. An increase of temperature to 55 °C hardly increases the relative intensity of the weak red emission. Shown in Figure 12 is an attempted spectral deconvolution. The emission spectrum at high CO<sub>2</sub> density (20.5 mol/dm<sup>3</sup>) was resolved into the LE band and a Gaussian with its maximum at  $26800 \text{ cm}^{-1}$  and  $\text{fwhm} = 6520 \text{ cm}^{-1}$ . While it is quite possible that the weak emission at high CO<sub>2</sub> density is indeed from the TICT state of DMABN, represented by the Gaussian in Figure 12, the small fractional contribution even at the highest density ( $\sim 8\%$ ) and the relatively large fitting residue prevent us from making a definite conclusion.

**DMAEB in Ethane.** The absorption and fluorescence spectra of DMAEB at low and high densities at 34.8 °C are shown in Figure 2C. The absorption maximum shifts to the red with increasing density also in the same very characteristic way, as was observed in CHF<sub>3</sub> and CO<sub>2</sub>. Figure 13 is a comparison of the density dependence of the absorption bathochromic shifts in CHF<sub>3</sub>, CO<sub>2</sub>, and ethane. The shifts in ethane are the least.

There are no TICT emissions in ethane at either 35 or 50 °C, nor are there shifts of the LE emission band. The fluorescence spectra of DMAEB in ethane at both temperatures are essentially independent of the fluid density.

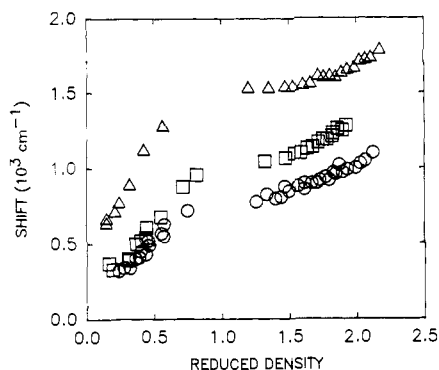


**Figure 13.** A comparison for the absorption bathochromic spectral shifts of DMAEB in  $\text{CHF}_3$  at 30.0 °C ( $\Delta$ ), in  $\text{CO}_2$  at 33.8 °C ( $\square$ ), and in ethane at 34.9 °C ( $\circ$ ).

## Discussion

**Bathochromic Shifts.** It is very interesting to see that all the dependencies of the bathochromic shifts on solvent density reported here follow a single characteristic pattern, despite the differences in the absolute magnitude of the observed shift from solvent to solvent. After a rapid change in the low-density region, a plateau appears under conditions near the critical density, followed by a second slower change in the high-density region. It is therefore important to recognize that the critical density is truly critical for the solvatochromic effects in a supercritical fluid in the sense that it represents the turning point from the strong density effects in the gaslike region of a supercritical fluid to the weaker effects in the liquidlike region. Our experimental results strongly suggest that the characteristic pattern of density dependence of bathochromic shifts is dictated primarily by the solvent properties at the near critical density region. The solute-solvent interactions influence the magnitude of the shift, but have little effect on the shape of the density dependence. In fact, for different solute probes (DMABN and DMAEB) the bathochromic shifts are nearly the same for a given fluid, in both absorption and emission.

The model for the characteristic solvatochromism in a supercritical fluid apparently consists of three regions exhibiting gas-phase solute-solvent clustering, clustering in the near-critical region, and "liquidlike" solvation. At low densities in the gas phase, the addition of each solvent molecule to the solvation shell causes a large incremental effect on solvatochromism. It is not surprising that the dielectric continuum theory does not describe this discrete process. These discrete solute-solvent interactions are quite different for  $\text{CHF}_3$ ,  $\text{CO}_2$ , and ethane, which is to be expected for these gas-phase clusters. Further evidence for gas-phase clusters is that radial distribution functions for nonpolar mixtures deviate from random behavior to a greater extent in the gas phase than at higher densities. In the other limit at liquidlike densities, the small bathochromic shifts reflect density effects on solvated solute molecules, which should follow the Onsager reaction field model.<sup>19,20</sup> These two regions will be used to provide a basis to explain the complex plateau region near the critical density.

At the highest densities in the Onsager continuum region, the shifts decrease essentially linearly with density. As the density decreases toward the critical point, the red shifts become greater than expected on the basis of extrapolation from the high-density region. This excess solvation has been observed in several systems with both absorption and fluorescence probes,<sup>2,7,8,11,21</sup> and with computer simulation,<sup>16,38,39</sup> and has been used to determine local densities. This local density augmentation or clustering of the solvent about the solute is facilitated by the large free volume and isothermal compressibility of the near-critical solvent. The solvatochromic shift remains large as the bulk density is decreased in the plateau region, because the compressibility continues to grow, maintaining the clusters. Eventually, at low densities in the gas phase, the clusters disappear rapidly as each solvent

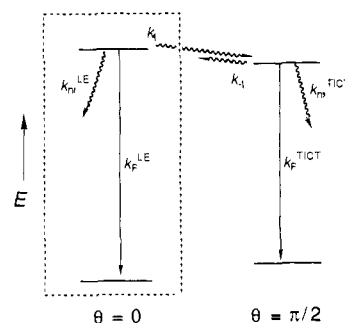


**Figure 14.** A kinetic scheme for TICT state formation in DMAEB and related molecules.

molecule is stripped from the solvation shell.

It is also instructive to examine the approach to the plateau region from low densities. As density is increased to  $\rho_r = 0.5$ , the shifts increase strongly as incremental solvent molecules are added to the solvation shell. At  $\rho_r = 0.5$ , the isothermal compressibility of the fluid is already quite large and the gas-phase clusters are sufficiently well developed to cause large solvatochromic shifts. As density is increased further, the effect is small in the plateau region. There appears to be a limit on how many solvent molecules the solute can attract in the cluster. Much larger pressures are required to raise the bulk density up to the local density of the cluster in the plateau region. Once this is accomplished, the bathochromic shifts continue to grow with density as shown in the high-density region.

Except in the low-density region, the density dependence of the solvent effects for different supercritical fluids are nearly the same. Especially worthy of notice is the dependence of  $x_{\text{TICT}}$  on solvent density. In  $\text{CHF}_3$  and  $\text{CO}_2$ , the contribution of the TICT state emission levels off after an initial rapid increase. Although  $x_{\text{TICT}}$  is only about 0.4 at the critical density of  $\text{CO}_2$  (less than half of that in  $\text{CHF}_3$ ), it increases only slightly upon further increase of  $\text{CO}_2$  density. This behavior again suggests the key interactions of solute-solvent molecules are those in the solvation shell.

This model predicts that clustering will be less pronounced at temperatures further away from the critical temperature. The temperature dependence of the solvatochromic shifts and the TICT state formation presented here are consistent with the expected trend, though a wider temperature range is required in order to make a stronger argument.

The observed clustering effects depend not only on the solvent character, but also on the nature of the solute probe. The effects on the highly polar TICT states are stronger than the effects on the less polar locally excited states. However, the difference again is greatest in the low-density region of the supercritical fluid.

**TICT State Formation in DMAEB.** The proposal<sup>33</sup> of two equilibrated 1:1 solute-solvent exciplexes for DMAEB in dioxane and polar solvents was designed primarily to account for the observed fluorescence lifetimes: 1.0 ns for the LE band in cyclohexane (the second emission band not present), 6.5 ns for both emission bands in dioxane, and 3.6 ns for both emission bands in propionitrile. The same fluorescence lifetime for two emission bands certainly suggests a thermodynamic equilibrium between the two emitting states. However, the longer lifetime in dioxane or in a polar solvent such as propionitrile than in a nonpolar hydrocarbon solvent such as cyclohexane does not at all validate the assumption that the blue band in the dual fluorescence corresponds to an emitting species other than the LE state. In fact, these observations can be better understood in the framework of a unimolecular TICT state mechanism.

In nonpolar hydrocarbon solvents, the observed fluorescence lifetime represents the decay processes of the locally excited state in the absence of the twisting and charge transfer pathway

$$\tau_{\text{F}}^{\text{LE}} = 1/(k_{\text{F}}^{\text{LE}} + k_{\text{nr}}^{\text{LE}} + k_{\text{t}}) \quad (3)$$

where  $k_{\text{F}}^{\text{LE}}$  and  $k_{\text{nr}}^{\text{LE}}$  are the rate constants of fluorescence and the overall nonradiative processes, respectively. An additional term,  $k_{\text{t}}$ , involving twisting can be neglected in nonpolar solvents. In

(38) DeBenedetti, P. G.; Kumar, S. K. *AIChE J.* **1988**, *34*, 645.

(39) DeBenedetti, P. G.; Mohamed, R. S. *J. Chem. Phys.* **1989**, *90*, 4528.

dioxane or polar solvents, the mechanism can be represented by the simplified kinetic scheme shown in Figure 14. The part of the scheme surrounded by a dashed line is used to illustrate the initial excited-state processes, among which the rate of twisting in the locally excited state  $k_t$  dominates its decay. The lifetime of the prompt fluorescence becomes much shorter and temperature dependent. A recent study of the temperature dependence of DMABN fluorescence lifetime in toluene<sup>40</sup> is fully consistent with this mechanism. After the initial decay, the locally excited state is repopulated thermally by the TICT state ( $k_{-1}$ ) and a thermodynamic equilibrium between the locally excited state and the TICT state is established. Therefore, the "delayed" fluorescence of the locally excited state and the emission of the TICT state have the same lifetime, as observed. The prompt fluorescence of DMAEB in dioxane and propionitrile at room temperature must be too short lived<sup>40,41</sup> to be detected by the spectrometer used for the lifetime measurements in ref 33.

The behavior of DMAEB in supercritical fluids is also unlikely to derive from two 1:1 solute-solvent exciplexes. In CO<sub>2</sub>, the LE band shifts bathochromically with increasing density, but its shape hardly changes at all, making it unlikely that an exciplex is formed. As discussed in the previous section, the characteristic solvent density dependence of bathochromic shifts for both the LE band and the TICT band also suggests a characteristic solvation process, rather than 1:1 exciplex formation.

**A Comparison between DMAEB and DMABN.** It has been proposed that the structures of the low-lying excited states in DMAEB and DMABN are different, primarily on the basis of the polarized spectroscopic studies at low temperature.<sup>18,25</sup> In DMABN, the lowest excited singlet state <sup>1</sup>B\* (S<sub>1</sub>) does not carry much transition probability. Instead, the <sup>1</sup>A\* state (S<sub>2</sub>) that is higher than <sup>1</sup>B\* is responsible for the absorption. The emission is presumably from the lowest <sup>1</sup>B\* state, naturally with a large Stokes shift. The emission could also be from equilibrated S<sub>1</sub> and S<sub>2</sub> states because of their small energy differences, according to a recent CNDO-S/CI calculation.<sup>42</sup> It has been shown<sup>40</sup> that there is an energy barrier between the locally excited state and the TICT state along the twisting coordinate, but it is not clear whether the barrier is due to diabatic crossing or due to the S<sub>1</sub>-S<sub>2</sub> energy gap and an intrinsic barrier on the S<sub>2</sub> energy surface. In DMAEB, the <sup>1</sup>A\* state is believed to be lower than the <sup>1</sup>B\* state, corresponding to a smaller Stokes shift, and the TICT state is formed adiabatically. Despite these differences, the observed density dependencies of absorption spectral bathochromic shifts in DMABN and DMAEB are nearly identical, indicating that the transitions in the two molecules are indeed of the same character.

The bathochromic shifts of the LE emission bands in DMABN and DMAEB are also very similar, although the emitting states in the two molecules are assumed to be different. It is likely that the <sup>1</sup>B\* state in DMABN borrows transition probability from the <sup>1</sup>A\* state, so the solvent effects on the <sup>1</sup>A\* state must have been borrowed as well. Since the bathochromic shifts of the LE band are small, it is hard to distinguish minor differences between the two molecules.

In CO<sub>2</sub>, significant TICT state emission was observed for DMAEB, but not for DMABN. This is consistent with observations in liquid solvents.<sup>18</sup> It is likely that in DMAEB the formation of the TICT state is an adiabatic process on the <sup>1</sup>A\* surface, while in DMABN it involves a <sup>1</sup>B\* to <sup>1</sup>A\* crossing. In CHF<sub>3</sub>, the increase of the fractional contribution of the TICT state emission with increasing solvent density is also faster in DMAEB than in DMABN.<sup>4</sup>

**A Comparison between Absorption and Emission.** The significant difference between solvent effects on absorption and on emission is interesting. It raises questions about previous treat-

ments of solvatochromic effects on DMABN,<sup>4,9</sup> in which the absorption spectral bathochromic shifts were assigned exclusively to the difference between the dipole moment of the ground state and the excited state, with no change in molecular geometry being considered. If so, the bathochromic shifts in emission should be at least as large as those observed in absorption. In the context of the Onsager reaction field theory,<sup>19,20</sup> the solvent effect on the Stokes shift  $\Delta\bar{\nu}_s$  can be evaluated according to the Lippert-Mataga equation<sup>43,44</sup>

$$\Delta\bar{\nu}_s = \Delta\bar{\nu}_{s,0} + 2[(\mu_e - \mu_g)^2 / hca^3] \Delta f \quad (4)$$

where  $\Delta\bar{\nu}_{s,0}$  is the Stokes shift in the absence of a medium,  $a$  is the Onsager distance,  $\mu_e$  and  $\mu_g$  are the electric dipole moments of the locally excited state and the ground state, respectively, and  $\Delta f$  is a function of solvent dielectric constants. Since  $\Delta f$  increases with increasing supercritical fluid density, eq 4 predicts that the Stokes shift will also increase with density. Therefore, the observed decrease of the Stokes shift with increasing density suggests a more complicated picture about the solvatochromism of DMABN and DMAEB. It is likely that the shape of the potential energy surface of the locally excited state, perhaps even the ground state, also changes with solvent density. This change must be responsible for at least part of the observed absorption bathochromic spectral shifts. Since the emission in these molecules is expected to be from a relaxed excited state, the shift in emission spectra is probably a better measure for the actual solvent effects on the transition energy.

**Solvent Effects on the Excited-State Energy Surface.** The dipole moments of an excited molecule differ along the excited-state energy surface, corresponding to different twisted geometries. For example, dipole moments of the locally excited state and the TICT state are different. Therefore, the energy surface will not just move up or down with solvent density or polarity, but will change its shape as well.<sup>45</sup> For both DMABN<sup>4</sup> and DMAEB, the results show that the TICT states undergo much larger bathochromic shifts than the locally excited states, consistent with the highly polar nature of the TICT state. Since the locally excited state and the TICT state are in thermodynamic equilibrium, the equilibrium constant  $K$  can be written as

$$K = (\Phi_F^{\text{TICT}} / \Phi_F^{\text{LE}}) (k_F^{\text{TICT}} / k_F^{\text{LE}})^{-1} = (x_{\text{TICT}} / x_{\text{LE}}) (k_F^{\text{TICT}} / k_F^{\text{LE}})^{-1} \quad (5)$$

where  $x_{\text{TICT}}/x_{\text{LE}}$  is the observed fluorescence quantum yield ratio of the two emitting states and  $k_F^{\text{LE}}$  and  $k_F^{\text{TICT}}$  are fluorescence radiative rate constants of the locally excited state and the TICT state, respectively. The 0,0 transition at the perpendicular geometry is Franck-Condon forbidden, and the fluorescence spectrum of the TICT state is believed to be due to hot emission from upper vibrational levels.<sup>18</sup> Therefore

$$k_F^{\text{TICT}} = \sum_{j=0} k_{F_j}^{\text{TICT}} \exp(ih\nu/kT) \quad (6)$$

where  $k_{F_j}^{\text{TICT}}$  is the fluorescence radiative rate constant corresponding to vibrational level  $i$ , and  $\nu$  is the vibration frequency. The solvent effects on this equilibrium can be evaluated:

$$\ln(x_{\text{TICT}}/x_{\text{LE}}) = -\Delta H/RT + [\Delta S/R + \ln(k_F^{\text{TICT}}/k_F^{\text{LE}})] \quad (7)$$

The enthalpy difference  $\Delta H$  can be approximated by the 0,0 splitting of the two emission bands:

$$\Delta H = \bar{\nu}_{00}^{\text{TICT}} - \bar{\nu}_{00}^{\text{LE}} = (\bar{\nu}_{\text{max}}^{\text{TICT}} - \bar{\nu}_{\text{max}}^{\text{LE}}) + \Delta H_c \quad (8)$$

where  $\Delta H_c$  is a constant correcting the difference between the 0,0 splitting and the splitting of the spectral maxima. Equation 7 can therefore be rewritten as

$$\ln(x_{\text{TICT}}/x_{\text{LE}}) = (1/R) [(\bar{\nu}_{\text{max}}^{\text{LE}} - \bar{\nu}_{\text{max}}^{\text{TICT}})/T] + [\Delta S/R + \ln(k_F^{\text{TICT}}/k_F^{\text{LE}}) - \Delta H_c/RT] \quad (9)$$

(40) Leinhos, U.; Kuhnle, W.; Zachariasse, K. A. *J. Phys. Chem.* **1991**, *95*, 2013.

(41) Rulliere, C.; Crabowski, Z. R.; Dobkowski, J. *Chem. Phys. Lett.* **1987**, *137*, 408.

(42) Majumdar, D.; Sen, R.; Bhattacharyya, K.; Bhattacharyya, S. P. *J. Phys. Chem.* **1991**, *95*, 4324.

(43) Lippert, E. *Ber. Bunsen-Ges. Phys. Chem.* **1957**, *61*, 962.

(44) Mataga, N.; Kaifu, Y.; Koizumi, M. *Bull. Chem. Soc. Jpn.* **1956**, *29*, 115, 465.

(45) Hicks, J. M.; Vandersall, M. T.; Sitzmann, E. V.; Eisenthal, K. B. *Chem. Phys. Lett.* **1987**, *135*, 413.

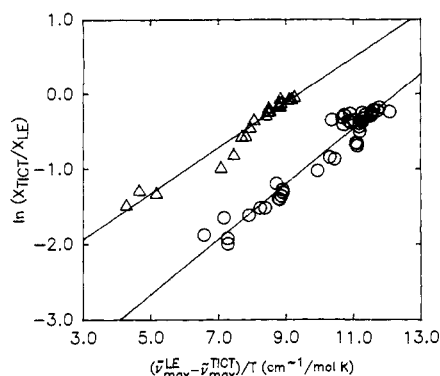


**Figure 15.** Dependence of the relative fluorescence quantum yields of the two emitting states on the energy difference between the TICT state and the LE state (eq 9) for DMAEB in  $\text{CO}_2$  at 33.8 °C (O) and 49.7 °C (Δ). The lines are the best linear least-squares fits with slope 0.367 and 0.303  $\text{mol K}/\text{cm}^{-1}$ , intercept  $-4.50$  and  $-2.83$ , and  $\gamma = 0.97$  and  $0.98$  for 33.8 and 49.7 °C, respectively.

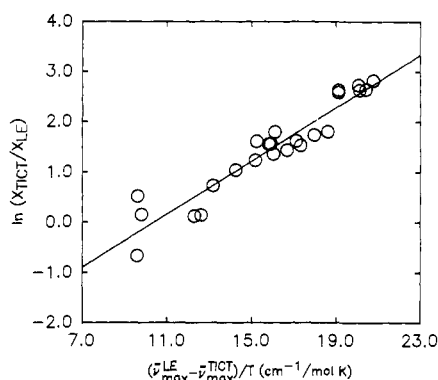


**Figure 16.** Dependence of the relative fluorescence quantum yields of the two emitting states on the energy difference between the TICT state and the LE state (eq 9) for DMAEB in  $\text{CHF}_3$  at 28.0 °C. The line is the best linear least-squares fit with slope 0.265  $\text{mol K}/\text{cm}^{-1}$ , intercept  $-2.75$ , and  $\gamma = 0.95$ .

Under the assumption that changes of entropy  $\Delta S$  and fluorescence rate constants  $k_{\text{F}}^{\text{TICT}}$  and  $k_{\text{F}}^{\text{LE}}$  with density are negligible, an isothermal plot of  $\ln(x_{\text{TICT}}/x_{\text{LE}})$  against  $(\bar{\nu}_{\text{max}}^{\text{TICT}} - \bar{\nu}_{\text{max}}^{\text{LE}})/T$  should be linear with a slope of  $1/R$  ( $1.439 \text{ mol K}/\text{cm}^{-1}$ ). The plots for DMAEB in  $\text{CO}_2$  at 33.8 and 49.7 °C are shown in Figure 15. They are almost linear, but the slopes ( $0.363$  and  $0.303 \text{ mol K}/\text{cm}^{-1}$  for low and high temperatures, respectively) are much smaller than  $1/R$ . A similar plot for DMAEB in  $\text{CHF}_3$  is shown in Figure 16. Again the slope  $0.265 \text{ mol K}/\text{cm}^{-1}$  is much smaller than  $1/R$ . The deviation probably derives from the entropy change and the density dependence of  $k_{\text{F}}^{\text{TICT}}$ . In addition, solvent effects on interactions between the LE state and TICT state, which can be more complicated than a simple equilibrium, may also lead to deviation from eq 5.

Since the volume of a solvated zwitterionic species, which is similar to a TICT state, decreases with improved solvation,<sup>46</sup> its entropy decreases as well. Likewise, the entropy of a TICT state should decrease as the solvent density increases. This effect is more pronounced for the TICT state than for the locally excited state, compensating for the change of enthalpy. Such a correlation

(46) Morais, J.; Ma, J.; Zimmt, M. B. *J. Phys. Chem.* **1991**, *95*, 3885.

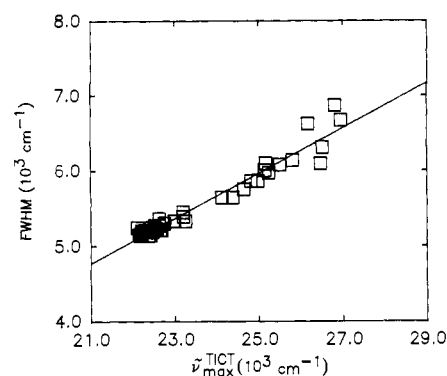


**Figure 17.** Correlation between the bathochromic shifts of the TICT band maximum and the bandwidth (fwhm) for DMAEB in  $\text{CHF}_3$  at 28.0 °C.

between the enthalpy change and the entropy change, known as the extrathermodynamic relationship, has also been observed in many other systems.<sup>47,48</sup>

It is likely that  $k_{\text{F}}^{\text{TICT}}$  also changes with density because of the change in  $\nu$  (eq 6). As the solvent density increases, stabilization of the TICT state is accompanied by increased curvature of the energy surface around the twisted geometry. Consequently, the energy gap  $h\nu$  increases and  $k_{\text{F}}^{\text{TICT}}$  decreases (eq 6).

Such an energy gap change also has an impact on the emission bandwidth. Isothermally, an increase in the energy gap will result in a decrease in the TICT emission bandwidth because fewer vibrational levels can be accessed. As shown in Figure 17 for DMAEB in  $\text{CHF}_3$ , the rapid decrease of the TICT band fwhm in the low-density region correlates well with the large bathochromic shifts of the TICT band maximum. The larger TICT emission bandwidths of DMAEB in  $\text{CO}_2$  than in  $\text{CHF}_3$  are consistent with the expectation. Another possibility is that the polydispersity of the clusters increases at low densities.<sup>11</sup>

Also consistent with this expectation is the effect of temperature on the bandwidth. The TICT emission bandwidths of DMAEB in  $\text{CO}_2$  at 49.7 °C are larger than those of 33.8 °C, apparently because the higher temperature allows access to more vibrational levels.

Finally, the special solvent effects of supercritical  $\text{CO}_2$  are somewhat ambiguous. Carbon dioxide is a nonpolar solvent and is of comparable polarizability to ethane, yet it causes significantly larger solvatochromic shifts than ethane for both DMABN and DMAEB and stabilizes the twisted excited state of DMAEB enough to favor the TICT state. Tentatively, we assume that this effect is related to the large quadrupole moment and the acidity of  $\text{CO}_2$ ,<sup>49</sup> but further investigation is required in order to make a definite assessment.

**Acknowledgment.** This research was supported by the National Science Foundation Grant No. CHE 90-17447 (M.A.F.), the Separations Research Program at the University of Texas, the State of Texas Energy Research in Applications Program, and the Camille and Dreyfus Foundation Teacher-Scholar Grant (K.P.J.). We thank J. Combes and K. E. O'Shea for their experimental assistance.

(47) Lefler, J. E.; Grunwald, E. *Rates and Equilibria of Organic Reactions*; John Wiley and Son: New York, 1963.

(48) Sun, Y.-P.; Saltiel, J.; Park, N. S.; Hoburg, E. A.; Waldeck, D. H. *J. Phys. Chem.* **1991**, in press.

(49) O'Shea, K. E.; Kirmse, K. M.; Fox, M. A.; Johnston, K. P. *J. Phys. Chem.* **1991**, in press.